



Published in final edited form as:

*Stroke*. 2012 December ; 43(12): 3258–3265. doi:10.1161/STROKEAHA.112.673400.

## Early Change in Ferumoxytol-Enhanced Magnetic Resonance Imaging Signal Suggests Unstable Human Cerebral Aneurysm. A Pilot Study

David Hasan, MD<sup>1</sup>, Nohra Chalouhi, MD<sup>2</sup>, Pascal Jabbour, MD<sup>2</sup>, Aaron S. Dumont, MD<sup>2</sup>, David K. Kung, MD<sup>1</sup>, Vincent A. Magnotta, PhD<sup>3</sup>, William L Young, MD<sup>4,5</sup>, Tomoki Hashimoto, MD<sup>5</sup>, H. Richard Winn, MD<sup>6</sup>, and Donald Heistad, MD<sup>7</sup>

<sup>1</sup>Department of Neurosurgery, Carver College of Medicine, University of Iowa, Iowa City, Iowa

<sup>2</sup>Department of Neurosurgery, Thomas Jefferson University and Jefferson Hospital for Neuroscience, Philadelphia, Pennsylvania

<sup>3</sup>Department of Radiology, Carver College of Medicine, University of Iowa, Iowa City, Iowa

<sup>4</sup>Department of Neurological Surgery, University of California San Francisco, San Francisco, California

<sup>5</sup>Department of Anesthesia and Perioperative Care, University of California San Francisco, San Francisco, California

<sup>6</sup>Department of Neurosurgery, Hofstra University and Lenox Hill Hospital, New York City, New York

<sup>7</sup>Departments of Internal Medicine and Pharmacology, Carver College of Medicine, University of Iowa, Iowa City, Iowa

### Abstract

**Background and Purpose**—The clinical significance of early (i.e. within the first 24 hours) uptake of ferumoxytol by macrophages in the wall of human cerebral aneurysms is not clear. The purpose of this study was to determine whether early uptake of ferumoxytol suggests unstable cerebral aneurysm.

**Methods**—Thirty unruptured aneurysms in 22 patients were imaged with MRI 24 hours after infusion of ferumoxytol. Eighteen aneurysms were also imaged 72 hours after infusion of ferumoxytol. Aneurysm dome tissue was collected from four patients with early MRI signal changes, five patients with late signal changes, and five other patients with ruptured aneurysms. The tissue was immunostained for expression of cyclooxygenase-1 (COX-1), cyclooxygenase-2 (COX-2), microsomal-prostaglandin-E2 synthase-1 (mPGES-1) and macrophages.

**Results**—In 23% (7/30) of aneurysms, there was pronounced early uptake of ferumoxytol. Four aneurysms were clipped. The remaining three aneurysms were managed conservatively; all three ruptured within six months. In 53% (16/30) of aneurysms, there was pronounced uptake of ferumoxytol at 72 hours. Eight aneurysms were surgically clipped and eight were managed conservatively; none ruptured or increased in size after six months. Expression of COX-2, mPGES-1, and macrophages was similar in unruptured aneurysms with early uptake of

---

Corresponding Author: David M Hasan, MD, Department of Neurosurgery, University of Iowa Hospitals and Clinics, 200 Hawkins Drive, JCP 1616, Iowa City, IA 52242, Ph: 319-384-8869, Fax: 319-353-6605, david-hasan@uiowa.edu.

**Conflict of interest/Disclosure**

None

ferumoxytol and ruptured aneurysms. Expression of these inflammatory molecules was significantly higher in aneurysms with early uptake of ferumoxytol versus aneurysms with late uptake.

**Conclusions**—Uptake of ferumoxytol in aneurysm walls within the first 24 hours strongly suggests aneurysm instability and probability of rupture within six months, and may warrant urgent intervention.

## Keywords

Aneurysm; MRI; Ferumoxytol; Rupture. Macrophages

## Introduction

Ferumoxytol (AMAG Pharmaceuticals, Lexington, MA), an iron oxide nanoparticle coated by a carbohydrate shell, is a member of the class of nanoparticles known as ultrasmall superparamagnetic particles of iron oxide (USPIOs). The drug was developed as a treatment for iron deficiency anemia in patients with chronic renal failure and was approved by the Food and Drug Administration in 2009.<sup>1–2</sup> Ferumoxytol is used in MRI studies for prolonged intravascular imaging. It also is useful as an inflammatory marker, when imaging is delayed because it is cleared by macrophages.<sup>3–4</sup> Ferumoxytol appears hypointense on MRI T2\* weighted gradient-echo (GE) sequences and can appear hyperintense on T1 weighted spin-echo sequences. The drug can be visualized intravascularly for up to 72 hours but begins to clear within 24 hours; delayed visualization (secondary to macrophage-uptake) occurs within 24 hours.

USPIO-enhanced MRI allows detection of phagocytic activity of inflammatory cells, such as macrophages. Several studies in experimental animals and humans have demonstrated that USPIO accumulates in atherosclerotic plaques in the abdominal aorta and internal carotid artery.<sup>5–11</sup> Thus, the method may allow noninvasive assessment of the inflammatory status of atherosclerotic lesions, and perhaps effects of anti-inflammatory pharmacological interventions on these lesions.<sup>5–11</sup>

We have demonstrated recently the feasibility of imaging macrophages within the wall of human cerebral aneurysms using ferumoxytol-enhanced MRI.<sup>12</sup> We also reported that imaging with T2\* gradient-echo MRI at 72 hours after infusion of 2.5–5 mg/kg of ferumoxytol provides optimal dose and timing parameters for imaging of macrophages within the aneurysm wall. The significance of early uptake (i.e. within the first 24 hours) of ferumoxytol however is not clear. We postulated that early uptake of ferumoxytol may indicate active inflammation in aneurysm walls and therefore unstable aneurysm. The current study correlates these imaging findings with the risk of intracranial aneurysm rupture.

## Methods

### Study Population

Patients with known unruptured untreated intracranial aneurysms, presenting to the Neurosurgery service at the University of Iowa Hospitals and Clinics, were prospectively enrolled in the study between January 2011 and June 2012. Five patients with ruptured intracranial aneurysms were enrolled for tissue analysis alone and did not undergo the imaging protocol. Exclusion criteria were age <18 years; pregnant women; history of allergy/hypersensitivity to iron, dextran, or iron-polysaccharide preparations; requirement for monitored anesthesia or IV sedation for MRI; contraindication to MRI; renal insufficiency, hepatic insufficiency or iron overload; and combination antiretroviral therapy.

The study protocol was approved by the University of Iowa Institutional Review Board and all enrolled patients provided written informed consent to participate in the study.

### MRI Protocol and Analysis

Ferumoxytol (2.5 – 5 mg/kg at a dilution of 30 mg/mL) was administered as a one-time dose to all patients with unruptured aneurysms enrolled in the study. A subset of these patients was used previously in establishing the feasibility of imaging macrophages in the wall of human cerebral aneurysms<sup>12</sup>. Safety data of the agent have been previously published<sup>8-9</sup> and the drug is commercially available as a treatment for iron-deficiency anemia. Off-label use of the drug in a research protocol was approved by the Institutional Review Boards at the University of Iowa and patients were monitored for adverse reactions to infusion of ferumoxytol. A Siemens 3T TIM Trio system was used for MRI. Patients completed a baseline MRI consisting of time-of-flight angiography and T2\* gradient-echo sequences. The time-of-flight angiographic sequence was collected using a 3D multi-slab technique with the following parameters: TE=3.6 ms, TR=20 ms, field-of-view =200×200×200 mm, matrix=384×384×20, bandwidth=165Hz/pixel. Four slabs were collected with a 20% overlap. The T2\* weighted sequence was collected using a 2D gradient-echo sequence with the following parameters: TE=20 ms, TR=500 ms, flip angle=20, FOV=220×220, matrix=512×384, slice thickness/gap=3.0/0.3 mm, bandwidth=260 Hz/pixel. The T1 weighted spin-echo images were collected using these parameters: TE=2.6ms, TR=317ms, flip angle=70°, FOV=220×220, Matrix=384×307, Bandwidth=330Hz/pixel, Averages=2, Slice thickness/gap=3.0/0.3mm. Imaging was performed at 4 times: Before infusion, immediately after infusion, and approximately 24 and 72 hours after infusion of ferumoxytol. Aneurysm size was measured using baseline CT angiogram (CTA), magnetic resonance angiogram (MRA), and/or digital subtraction diagnostic angiogram.

### Analysis

Images obtained before, immediately after, and 24- and 72-hours after infusion of ferumoxytol were compared. A loss of signal intensity (from pre-infusion to delayed post-infusion imaging) detected on T2\* weighted sequences (corresponding to extraluminal regions of the imaged lesions) was considered a positive finding. Post-infusion images were co-registered to the baseline images using a rigid transformation and a mutual information similarity metric. Histogram matching was then performed between the two datasets before the baseline image was subtracted from the post-infusion image (i.e., difference = post-infusion minus baseline). The difference image allowed demonstration of a relative signal change from baseline to post-infusion. Two neuroradiologists independently reviewed baseline, post-infusion, and subtracted images from all patients in a blinded fashion and rated the change in signal intensity (considered as consistent or inconsistent with uptake of ferumoxytol). The “percentage of agreement” and Kappa ( $\kappa$ ) estimate of agreement were used to calculate interobserver agreement.

### Histology of aneurysms

Fourteen patients underwent microsurgical clipping of their aneurysms. Aneurysm dome tissue was analyzed histologically (Figure 1). Four patients had unruptured aneurysms and uptake of ferumoxytol was measured within 24 hours of infusion; five patients had unruptured aneurysms and uptake of ferumoxytol was measured at 72 hours; and five patients had ruptured aneurysms. As explained above, the five patients with ruptured aneurysms did not undergo the imaging protocol.

Aneurysm tissues were immunostained with monoclonal antibodies to cyclooxygenase-1 (COX-1 [Epitomics, Burlington CA]), cyclooxygenase-2 (COX-2 [Epitomics, Burlington CA]), microsomal prostaglandin E2 synthase-1 (mPGES-1 [Cayman Chemical, Ann Arbor,

MIJ), M1 macrophages using anti-HLA DR for M1 (ABCAM, Cambridge MA), and M2 macrophages using anti-CD 163 for M2 (ABCAM, Cambridge MA).

Semiquantitative analysis of the slides was performed based on cell count (immunostained positive cells) per high-power field (HPF) (40X): grade 0= 0 cells per HPF, grade 1 = 0–10 cells per HPF, grade 2 = 10–20 cells per HPF and grade 3 = >20 cells per HPF. Assessment of slides stained for COX-1, COX-2, mPGES-1, M1 and M2 was made by an observer who was not aware of the source of tissues. Statistical analysis was performed using Kruskal-Wallis test, a nonparametric ANOVA test. P values < 0.05 were considered statistically significant.

## Results

Twenty-two patients harboring a total of 30 aneurysms completed the imaging study and were included in the imaging analysis protocol (Figure 1). Six patients were male and 16 were female. Eleven aneurysms were smaller than 7 mm and 19 were larger than 7 mm. Table 1 summarizes patient demographics, aneurysm characteristics, and imaging findings. No patient experienced ferumoxytol-related adverse events.

### Aneurysm Imaging

Thirty aneurysms were imaged and analyzed. There was early uptake of ferumoxytol on MRI in seven aneurysms (23%); no uptake on both early or late MRI in seven aneurysms (23%); and only late MRI signal change from uptake of ferumoxytol in 16 (53%) aneurysms (Figures 2). Six of 7 aneurysms with early signal changes were  $\leq$  7 mm and all those that ruptured were  $\geq$  15 mm (Figure 3). 94% of aneurysms with late signal change were < 15 mm. Sixteen aneurysms were observed and 14 were surgically clipped (4 aneurysms with early MRI signal changes, 8 aneurysms with late MRI signal changes, and 2 with no MRI signal changes). The decision to observe these 16 aneurysms was based on aneurysm size, patient's age, co-morbidities, and preferences.

Of the 16 aneurysms that were observed, 3 aneurysms had early signal changes, 8 aneurysms had only late signal changes, and in 5 there were no signal changes. All three aneurysms with early signal changes ruptured within a 6-month observation period. All three patients were female, and their aneurysms measured 14×15 mm, 35×30 mm, and 25×15 mm. Two of these patients were not operated on because of their age, and the high morbidity and mortality associated with a technically complex surgery. The third patient underwent stent-assisted coiling after aneurysm rupture. Of the 8 aneurysms with late uptake of ferumoxytol that were managed conservatively, none ruptured or increased in size based on follow-up MRA and/or CTA in the follow-up period.

Of the 30 aneurysms reviewed by two neuroradiologists, there was a lack of agreement about the MRI signal change for only one aneurysm. The interobserver agreement was found to be 95% using the “percentage of agreement” method and 92% using the Kappa (K) estimate of agreement.

### Histological Findings

COX-2, mPGES-1, and M1 cells were increased in ruptured aneurysms, and similar in magnitude to unruptured aneurysms with early MRI signal changes (Figures 4, 5). Expression of COX-2 and mPGES-1, and number of M1 cells was greater in unruptured aneurysms with early MRI signal changes than in unruptured aneurysms with late signal changes ( $p < 0.05$ ). Immunostaining of COX-1 and M2 were similar in the groups.

## Discussion

Substantial evidence suggests that inflammation is a key component in the pathophysiology of cerebral aneurysm formation and rupture.<sup>13</sup> Ferumoxytol-enhanced MRI is a non-invasive method for detection of the phagocytic activity of inflammatory cells in the walls of aneurysms using macrophages as a surrogate marker. The current study provides preliminary evidence that aneurysms with early uptake of ferumoxytol on MRI are prone to rupture and thus may warrant early operative intervention.

### Inflammation and Cerebral Aneurysms

In response to hemodynamic stress, endothelium undergoes several proinflammatory changes<sup>14</sup> including activation of nuclear factor kappa B (NF- $\kappa$ B),<sup>15</sup> monocyte chemoattractant protein 1 (MCP-1)<sup>16–17</sup> and vascular cell adhesion molecule 1 (VCAM-1).<sup>18–19</sup> These molecules are highly chemotactic to macrophages and other inflammatory cells.

Macrophages play a crucial role in the pathogenesis of cerebral aneurysms.<sup>13, 20</sup> Macrophage depletion and knockout of the MCP-1 gene reduce the incidence of cerebral aneurysms in mice.<sup>20</sup> Macrophages, which have also been observed in the wall of intracranial aneurysms in rats, secrete extra cellular matrix-degrading proteolytic enzymes and induce apoptosis of smooth muscle cells.<sup>13, 20</sup> Macrophages are an important source of matrix metalloproteinases 2 and 9, which presumably decrease the mechanical strength of aneurysms and contribute to their rupture.<sup>13</sup> COX-2, mPGES-1 and prostaglandin E receptor 2 are induced in endothelial cells of cerebral aneurysms.<sup>21</sup> Suppression of NF- $\kappa$ B-mediated chronic inflammation reduces the incidence of cerebral aneurysm in rats.<sup>15</sup> We have recently demonstrated that expression of COX-2 and mPGES-1 is increased in the walls of human cerebral aneurysms, and that expression of these molecules is greater in ruptured than in unruptured aneurysms.<sup>22</sup>

In summary, studies in both human and experimental animal suggest an important role of macrophages and inflammation in the pathophysiology of intracranial aneurysms.

### MRI signals versus risk of rupture of aneurysms

Aneurysms may show early signal changes (within the first 24 hours), late signal changes (at 72 hours post infusion), or no signal changes on MRI T2\* GE, depending on the uptake of ferumoxytol nanoparticles by macrophages localized in their walls. This study suggests that aneurysms with early MRI changes have a higher risk of rupture, as compared to aneurysms with late or no signal changes. Interestingly, the size of aneurysms with early MRI signal changes was variable (6/7 aneurysms were 7 mm and aneurysms that ruptured were 15 mm), and they did not cluster in a specific location. The sample is too small, however, to draw a strong conclusion that the intensity of the inflammatory response in the aneurysm wall is independent of aneurysm size and location. These two factors are major determinants of the risk of aneurysm rupture.<sup>23</sup>

Early MRI signal changes noted on T2\*GE sequence are produced by increased uptake of ferumoxytol nanoparticles by macrophages that are localized within aneurysm walls. Early uptake therefore suggests an active inflammatory process. Indeed, this hypothesis was confirmed histologically, as inflammatory cells and molecules (COX-2, mPGES-1, and macrophages) were found to be markedly upregulated in aneurysms with early signal changes. Importantly, expression of these molecules was significantly higher in aneurysms with early MRI changes versus aneurysms with late or no MRI changes. Furthermore, expression of inflammatory molecules and cells was similar in unruptured aneurysms with early signal changes and ruptured aneurysms; this finding strongly suggests that aneurysms

with early signal changes are unstable lesions with high risk of rupture, when we did not intervene early. The finding that all three aneurysms with early signal changes that were managed conservatively progressed to rupture in less than 6 months further supports this hypothesis.

These observations support the hypothesis that inflammation is an important cause of aneurysm rupture, rather than a consequence of rupture. Previous studies that reported inflammatory changes in the walls of ruptured aneurysms fell short of demonstrating that the inflammatory response was present before rupture of aneurysms, as opposed to a response to aneurysm rupture<sup>13</sup>. We thus provide the first direct evidence that inflammation is a causal factor in progression of cerebral aneurysms in humans to rupture.

If the findings of this preliminary report are validated in a larger study, ferumoxytol-enhanced MRI could be applied in clinical practice as a non-invasive tool to differentiate “unstable” aneurysms that require early intervention from “stable” aneurysms in which observation may be safe. Specifically, this technique could prove particularly useful in identifying rupture-prone aneurysms in patients that often pose a therapeutic dilemma, namely elderly patients (> 70 years old) and patients harboring small aneurysms (< 7 mm).<sup>23</sup>

### Limitations

The relatively small number of patients enrolled and the short follow-up period are limitations of this study. Sufficient data were obtained however to reveal consistent patterns of labeling and demonstrate the potential clinical utility of this method. Longer follow-up periods are necessary to determine the natural history of aneurysms with late signal changes, and the ability of ferumoxytol-enhanced MRI to determine whether there is progression of these “stable” aneurysms to an unstable phenotype that is prone to rupture.

### Summary

Unstable aneurysms, suggested by early uptake of ferumoxytol in aneurysm walls within the first 24 hours and inflammation, are generally large and warrant early intervention. This novel MRI technique holds promise for patients harboring unruptured cerebral aneurysms. In addition, histological findings support the hypothesis that inflammation plays an integral part in progression of aneurysms to rupture. Larger clinical studies are needed to validate these observations.

### Acknowledgments

We are grateful to Wendy Smoker, MD and Bruno Policeni, MD (University of Iowa, Carver College of Medicine, Department of Neuroradiology) for reviewing all images for the study. We would also like to thank Christine Hochstedler for helping with the histology slides for the study.

#### Funding

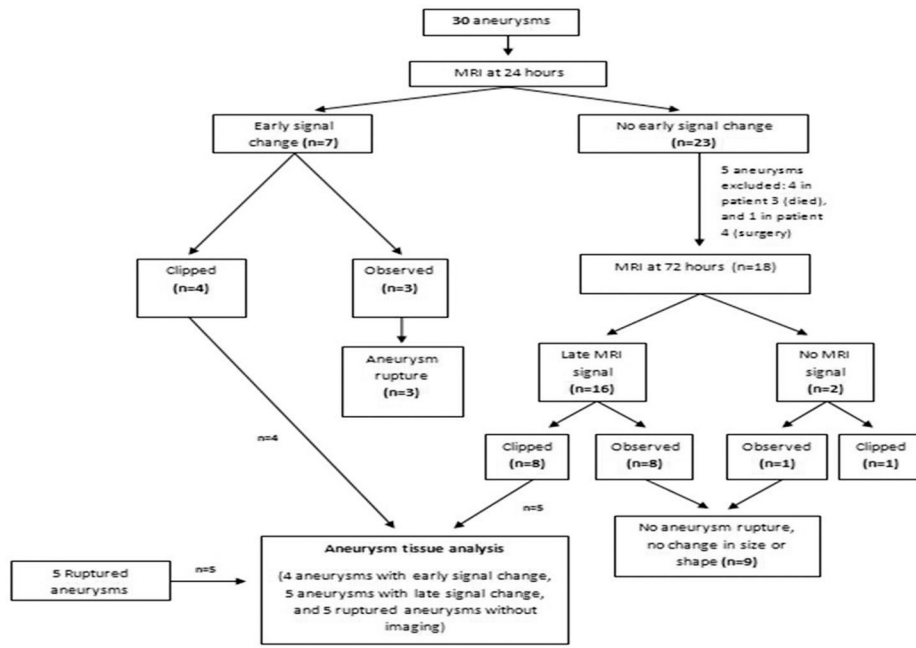
This study was supported by NIH grant # R03NS07922 (and the Brain Aneurysm Foundation) to D. Ha. No funding was provided by AMAG. Pharmaceuticals Inc, the manufacturer of ferumoxytol.

### References

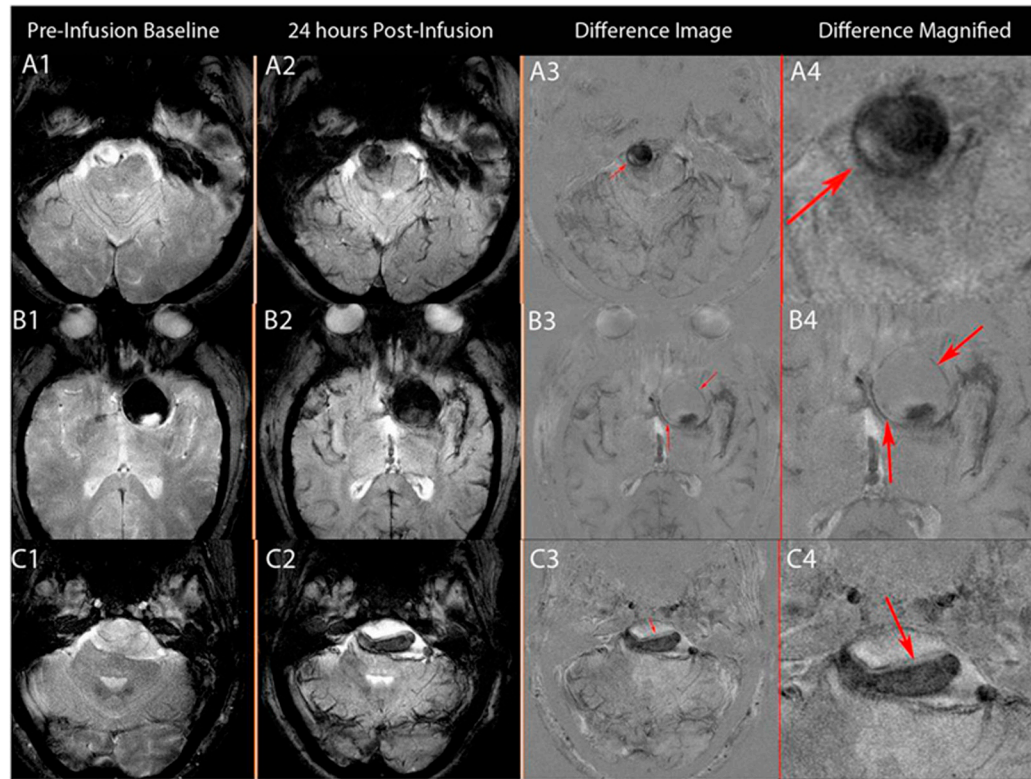
1. Lu M, Cohen MH, Rieves D, Pazdur R. Fda report: Ferumoxytol for intravenous iron therapy in adult patients with chronic kidney disease. *Am J Hematol*. 2010; 85:315–319. [PubMed: 20201089]
2. Spinowitz BS, Kausz AT, Baptista J, Noble SD, Sothinathan R, Bernardo MV, et al. Ferumoxytol for treating iron deficiency anemia in ckd. *J Am Soc Nephrol*. 2008; 19:1599–1605. [PubMed: 18525001]

3. Dosa E, Tuladhar S, Muldoon LL, Hamilton BE, Rooney WD, Neuwelt EA. Mri using ferumoxytol improves the visualization of central nervous system vascular malformations. *Stroke*. 2011; 42:1581–1588. [PubMed: 21493906]
4. Neuwelt EA, Varallyay CG, Manninger S, Solymosi D, Haluska M, Hunt MA, et al. The potential of ferumoxytol nanoparticle magnetic resonance imaging, perfusion, and angiography in central nervous system malignancy: A pilot study. *Neurosurgery*. 2007; 60:601–611. discussion 611-602. [PubMed: 17415196]
5. Herborn CU, Vogt FM, Lauenstein TC, Dirsch O, Corot C, Robert P, et al. Magnetic resonance imaging of experimental atherosclerotic plaque: Comparison of two ultrasmall superparamagnetic particles of iron oxide. *J Magn Reson Imaging*. 2006; 24:388–393. [PubMed: 16791857]
6. Hyafil F, Laissy JP, Mazighi M, Tchetché D, Louedec L, Adle-Biassette H, et al. Ferumoxtran-10-enhanced mri of the hypercholesterolemic rabbit aorta: Relationship between signal loss and macrophage infiltration. *Arterioscler Thromb Vasc Biol*. 2006; 26:176–181. [PubMed: 16269663]
7. Ruehm SG, Corot C, Vogt P, Kolb S, Debatin JF. Magnetic resonance imaging of atherosclerotic plaque with ultrasmall superparamagnetic particles of iron oxide in hyperlipidemic rabbits. *Circulation*. 2001; 103:415–422. [PubMed: 11157694]
8. Trivedi RA, UK-I JM, Graves MJ, Cross JJ, Horsley J, Goddard MJ, et al. In vivo detection of macrophages in human carotid atheroma: Temporal dependence of ultrasmall superparamagnetic particles of iron oxide-enhanced mri. *Stroke*. 2004; 35:1631–1635. [PubMed: 15166394]
9. Trivedi RA, UK-I JM, Graves MJ, Kirkpatrick PJ, Gillard JH. Noninvasive imaging of carotid plaque inflammation. *Neurology*. 2004; 63:187–188. [PubMed: 15249641]
10. Weinstein JS, Varallyay CG, Dosa E, Gahramanov S, Hamilton B, Rooney WD, et al. Superparamagnetic iron oxide nanoparticles: Diagnostic magnetic resonance imaging and potential therapeutic applications in neurooncology and central nervous system inflammatory pathologies, a review. *J Cereb Blood Flow Metab*. 2010; 30:15–35. [PubMed: 19756021]
11. Yancy AD, Olzinski AR, Hu TC, Lenhard SC, Aravindhan K, Gruver SM, et al. Differential uptake of ferumoxtran-10 and ferumoxytol, ultrasmall superparamagnetic iron oxide contrast agents in rabbit: Critical determinants of atherosclerotic plaque labeling. *J Magn Reson Imaging*. 2005; 21:432–442. [PubMed: 15779033]
12. Hasan DM, Mahaney KB, Magnotta VA, Kung DK, Lawton MT, Hashimoto T, et al. Macrophage imaging within human cerebral aneurysms wall using ferumoxytol-enhanced mri: A pilot study. *Arterioscler Thromb Vasc Biol*. 2012; 32:1032–1038. [PubMed: 22328774]
13. Chalouhi N, Ali MS, Jabbour PM, Tjoumakaris SI, Gonzalez LF, Rosenwasser RH, et al. Biology of intracranial aneurysms: Role of inflammation. *Journal of Cerebral Blood Flow & Metabolism*. 2012; 32:1659–1676. [PubMed: 22781330]
14. Chien S. Effects of disturbed flow on endothelial cells. *Ann Biomed Eng*. 2008; 36:554–562. [PubMed: 18172767]
15. Aoki T, Kataoka H, Shimamura M, Nakagami H, Wakayama K, Moriwaki T, et al. Nf-kappab is a key mediator of cerebral aneurysm formation. *Circulation*. 2007; 116:2830–2840. [PubMed: 18025535]
16. Aoki T, Kataoka H, Ishibashi R, Nozaki K, Egashira K, Hashimoto N. Impact of monocyte chemoattractant protein-1 deficiency on cerebral aneurysm formation. *Stroke*. 2009; 40:942–951. [PubMed: 19164781]
17. Krischek B, Kasuya H, Tajima A, Akagawa H, Sasaki T, Yoneyama T, et al. Network-based gene expression analysis of intracranial aneurysm tissue reveals role of antigen presenting cells. *Neuroscience*. 2008; 154:1398–1407. [PubMed: 18538937]
18. Kosierkiewicz TA, Factor SM, Dickson DW. Immunocytochemical studies of atherosclerotic lesions of cerebral berry aneurysms. *J Neuropathol Exp Neurol*. 1994; 53:399–406. [PubMed: 8021714]
19. Shi C, Awad IA, Jafari N, Lin S, Du P, Hage ZA, et al. Genomics of human intracranial aneurysm wall. *Stroke*. 2009; 40:1252–1261. [PubMed: 19228845]
20. Kanematsu Y, Kanematsu M, Kurihara C, Tada Y, Tsou TL, van Rooijen N, et al. Critical roles of macrophages in the formation of intracranial aneurysm. *Stroke*. 2011; 42:173–178. [PubMed: 21106959]

21. Aoki T, Nishimura M, Matsuoka T, Yamamoto K, Furuyashiki T, Kataoka H, et al. Pge(2) -ep(2) signalling in endothelium is activated by haemodynamic stress and induces cerebral aneurysm through an amplifying loop via nf-kappab. *Br J Pharmacol*. 2011; 163:1237–1249. [PubMed: 21426319]
22. Hasan D, Hashimoto T, Kung D, Macdonald RL, Winn HR, Heistad D. Upregulation of cyclooxygenase-2 (cox-2) and microsomal prostaglandin e2 synthase-1 (mpges-1) in wall of ruptured human cerebral aneurysms: Preliminary results. *Stroke*. 2012; 43:1964–1967. [PubMed: 22588264]
23. Chalouhi N, Dumont AS, Randazzo C, Tjoumakaris S, Gonzalez LF, Rosenwasser R, et al. Management of incidentally discovered intracranial vascular abnormalities. *Neurosurg Focus*. 2011; 31:E1. [PubMed: 22133178]



**Figure 1.** Schematic presentation of the study.



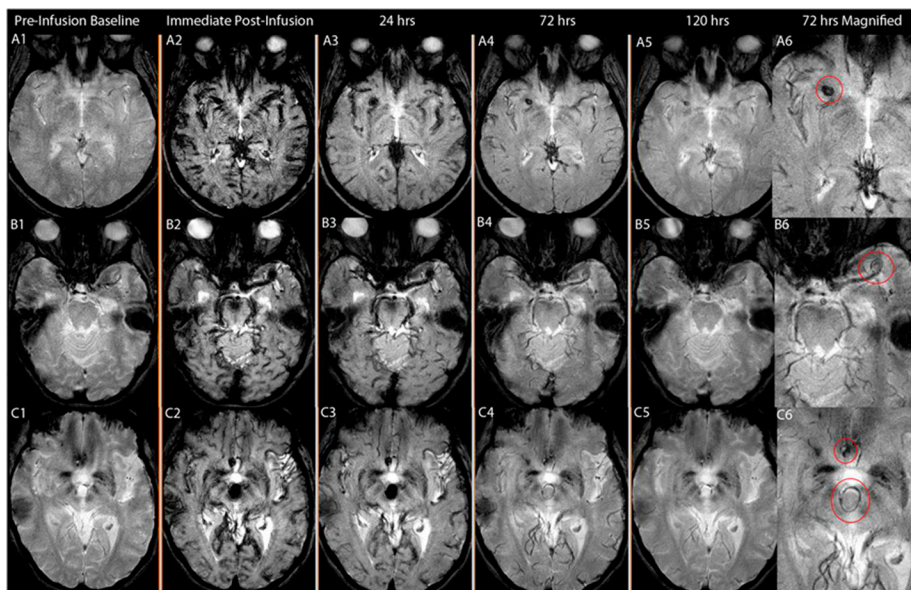
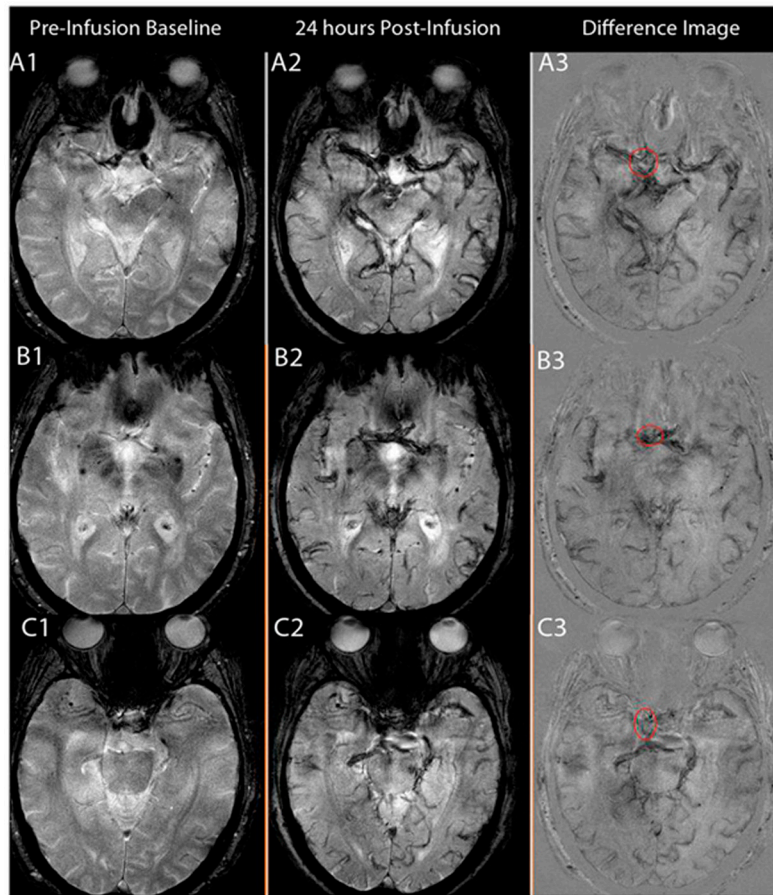


**Figure 2.**  
**Figure 2(A-B-C): A:** T2\* GE MRI sequence at baseline and 24 hours post-infusion showing early signal changes in the walls of three cerebral aneurysms (Panel A1–4 corresponds to patient # 1 with a right vertebral artery aneurysm, panel B1–4 corresponds to patient # 2

with a left supraclinoid ICA aneurysm, and panel C1–4 corresponds to patient # 3 with a fusiform vertebrobasilar artery aneurysm). Difference images (last two panels) demonstrate the relative signal loss after ferumoxytol infusion. All three aneurysms ruptured within six months. **B:** T2\* GE MRI sequence at baseline and 24 hours post-infusion, and subtraction images showing no early signal changes in three aneurysms from patient # 3 (Panel A 1–3, right ICA terminus aneurysm; panel B 1–3, anterior communicating artery aneurysm; and panel C 1–3, right cavernous ICA aneurysm). None of these aneurysms ruptured during the follow-up period. **C:** T2\* GE MRI sequence at five different times and magnified subtraction image at 72- hours post – infusion, showing late MRI signal changes in three aneurysms. Panel A 1–6 corresponds to patient # 8 with a right middle cerebral artery aneurysm, panel B 1–6 corresponds to patient # 19 with a left middle cerebral artery aneurysm, and panel C 1–6 corresponds to patient # 9 with anterior communicating artery and basilar tip aneurysms (the left middle cerebral artery aneurysm was on a different cut). MRI signal changes are best detected in the wall of these aneurysms at 72 hours post-infusion of ferumoxytol. None of these aneurysms ruptured during the follow-up period.

\$watermark-text

\$watermark-text

\$watermark-text

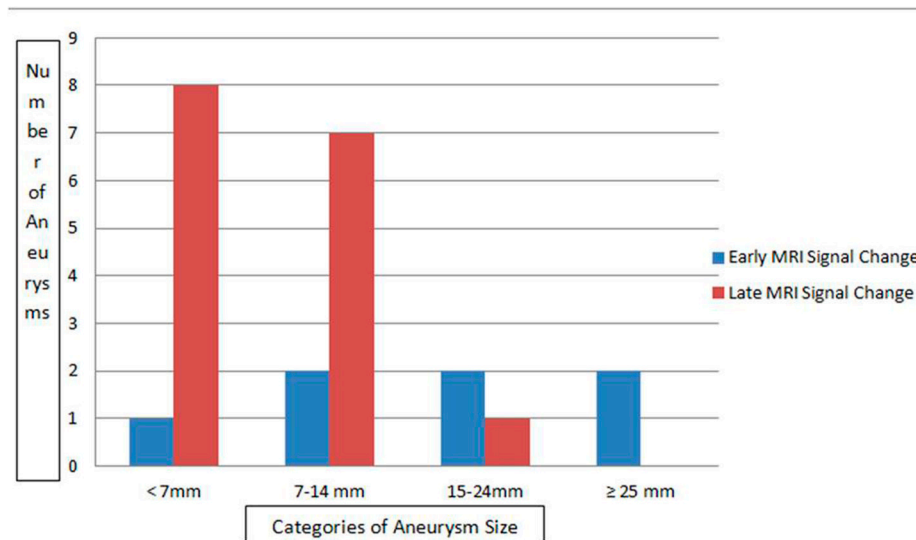


**Figure 3.** Distribution of aneurysms with early MRI signal change vs. late MRI signal change in relation to aneurysm size. Early MRI signal change was independent of aneurysm size. Late MRI signal change was noted in 50% of aneurysms < 7mm, and 44% in aneurysms 7–14mm.

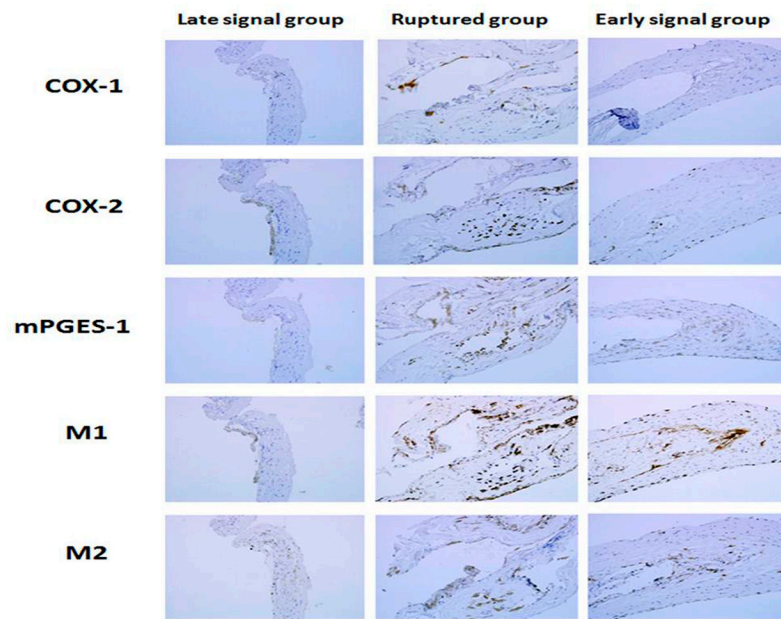


**Figure 4.**

Immunostaining for three different aneurysm categories: Aneurysms with late MRI signal changes, ruptured aneurysms, and aneurysms with early MRI signal changes.

Immunostaining for COX-1 and M2 cells is similar in the three categories of aneurysms. Immunostaining for COX-2, mPGES-1, and M1 cells indicates upregulation in aneurysms with early MRI signal changes in a similar manner to ruptured aneurysms.

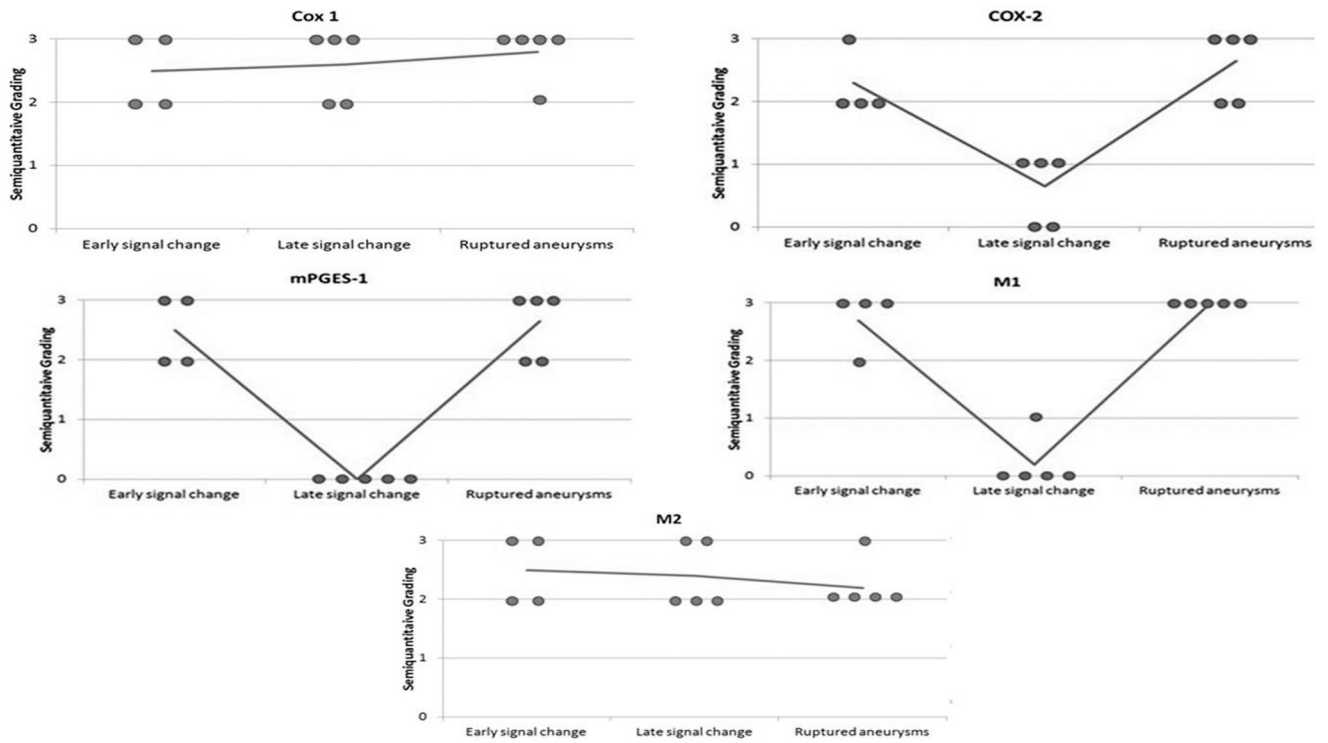


**Figure 5.** Semiquantitative grading for tissues collected from aneurysms with early MRI signal changes (n=4), aneurysms with late MRI signal changes (n=5), and ruptured aneurysms (n=5). Immunostaining for COX-1 and M2 cells is similar in the three categories of aneurysms. Immunostaining for COX-2, mPGES-1, and M1 cells indicates upregulation in aneurysms with early MRI signal changes in a similar manner to ruptured aneurysms.

**Table 1**

Patient demographics, aneurysm characteristics, and imaging findings

Pt. No.	Age (yrs)	Sex	Location*	Size (mm)	Observations vs. Surgery	Rupture
<b>Early uptake</b>						
1	75	F	R Vertebral	14×15	observation	yes
2	50	F	L ICA	35×30	observation	yes
3	76	F	Fusiform vertborbasilar	26×15	observation	yes
4	62	F	R Pcomm	6×4	surgery	no
5	52	F	L MCA	12×9	surgery	no
6	55	F	R ophthalmic	10×7	surgery	no
7	52	F	L MCA	7×5	surgery	no
<b>Late uptake</b>						
8	67	F	R MCA	6×5	surgery	no
9	77	F	Basilar tip	18×14	observation	no
9	77	F	L MCA	4×5	observation	no
9	77	F	Acomm	3×3	observation	no
10	78	F	Basilar tip	18×14	observation	no
11	68	M	L MCA	5×4	surgery	no
11	68	M	R MCA	9×6	surgery	no
12	68	F	Acomm	5×5	observation	no
13	44	F	L MCA	4×5	observation	no
14	38	F	Basilar tip	4×6	observation	no
15	47	M	R pcomm	14×11	surgery	no
16	67	F	R MCA	7×8	surgery	no
17	50	F	L ICA	9×6	surgery	no
18	56	M	R MCA	5×4	surgery	no
19	52	F	L MCA	10×10	surgery	no
20	71	M	R MCA	6×8	observation	no
<b>No uptake</b>						
3	76	F	R cavernous	15×11	observation	no

Pt. No.	Age (yrs)	Sex	Location*	Size (mm)	Observations vs. Surgery	Rupture
3	76	F	R ICA terminus	4×2	observation	no
3	76	F	L paracliniod	6×5	observation	no
3	76	F	A comm	8×8	observation	no
21	56	F	R MCA	7×8	surgery	no
22	44	M	R MCA	10×10	surgery	no
10	78	F	L MCA	9×10	observation	no

\* R = Right, L = Left, ICA = Internal Carotid Artery, Acomm = Anterior Communicating Artery, Pcomm = Posterior Communicating Artery, MCA = Middle Cerebral Artery,